The Bioscan
AN INTERNATIONAL QUARTERLY JOURNAL OF LIFE SCIENCES
20(3): S.I (3), 568-573, 2025 www.thebioscan.com

A COMPREHENSIVE ASSESSMENT ON THE CHARACTERISTICS OF CELLULOSE ACETATE/SODIUM ALGINATE BIO COMPOSITES AND ITS ANTI MICROBIAL ACTIVITY

[1]M. Sreetha, [2]G.R. Bella

[1]Research scholar, Department of Chemistry and Research Centre,Scott Christian College, (Autonomous), Nagercoil-629003
(Affiliated to Manonmanium Sundaranar University,
Tirunelveli-627 012, Tamil Nadu, India)

[2]Research supervisor and Assistant professor, Department of Chemistry and Research Centre, Scott Christian College, (Autonomous), Nagercoil-629003
(Affiliated to Manonmanium Sundaranar University,
Tirunelveli-627 012, Tamil Nadu, India)

[2]Email id: grbella321@gmail.com

DOI: 10.63001/tbs.2025.v20.i03.S.I(3).pp568-573

KEYWORDS
bio composite, green chemistry, natural polymer, solvent casting, sustainable resources
Received on:

19-06-2025

Accepted on:

16-07-2025

Published on:

21-08-2025

ABSTRACT

Cellulose derivatives and their associated polymers represent a cornerstone of sustainable materials and contribute substantially to advancements in green chemistry. In the present study, bio composites were developed by combining sodium alginate, a naturally occurring polysaccharide derived from seaweed with cellulose acetate, an ester derivative of cellulose. Among various fabrication techniques available for composite synthesis, solvent casting was selected due to its simplicity and for its cost effectiveness. To evaluate the physicochemical properties of the resulting bio composites, cellulose acetate and sodium alginate were blended in different ratios and subjected to comprehensive characterization. Surface morphology and structural properties were analysed using Fourier-transform infrared spectroscopy (FTIR), X-ray diffraction (XRD) and Scanning electron microscopy (SEM). FTIR spectra confirmed the formation of intermolecular crosslinking between cellulose acetate and sodium alginate, as evidenced by the presence of characteristic absorption bands corresponding to both components. XRD data clearly indicated that all four compositions exhibited an amorphous nature, as demonstrated by the crystallinity indices, which consistently suggested the presence of a predominantly disordered structural configuration across all samples and the crystallinity index of sodium alginate experienced a marked increase following the incorporation of cellulose acetate, indicating a significant enhancement in structural order. SEM analysis revealed the complete dispersion of cellulose acetate and sodium alginate to form a smooth surfaced film. Mechanical characterization indicated that the tensile strength of the fabricated bio composites ranged from 1 to 4 N/mm^2, reflecting moderate structural integrity suitable for potential biomedical and packaging applications. Furthermore, antimicrobial assays demonstrated that while cellulose acetate alone exhibited no observable antimicrobial activity, the incorporation of sodium alginate imparted a modest enhancement in bioactivity. As a result, the resulting composites displayed pronounced inhibitory effects against the fungal strain *Aspergillus niger* and several pathogenic bacterial species, including *Klebsiella pneumoniae*, *Escherichia coli*, *Bacillus subtilis,* and *Staphylococcus albus,* thereby underscoring their potential as multifunctional biomaterials.

INTRODUCTION

The imperative transition from finite fossil fuels to sustainable materials has led to a growing interest in harnessing biomass and renewable resources for polymer production. Cellulose, with its immense natural abundance and annual production of 1.5×10^{12} tons, has emerged as a prime candidate for sustainable material development. Cellulose acetate (CA), a prominent derivative of cellulose, has been extensively utilized in various applications, including optical films, textile fibers, and cigarette filters, owing to its unique properties and versatility. By leveraging the potential of cellulose and its derivatives, researchers aim to create sustainable materials that can mitigate the environmental impact of traditional fossil fuel-based polymers [1-4]. Given its notable mechanical strength, CA stands out as a prominent cellulose

derivative, facilitating its processing from melts or solutions into various forms such as films, membranes, and fibers. This property enables the creation of diverse materials with tailored characteristics, making it a versatile and valuable material for a range of applications [5-7]. Extensive research has been conducted to further enhance the properties of cellulose acetate (CA) through the incorporation of various functional components, including bioactive nanofillers, antimicrobial essential oil nanocapsules, nanocomposites, and nanoparticles, with applications spanning food safety, biomedical packaging, and drug delivery systems [8-11].

Sodium alginate (SA), a naturally occurring polysaccharide, boasts a linear structure and water-holding capacity, rendering it a safe, biodegradable, and biocompatible material. Its unique properties, including gelling, viscosity, and stabilization, confer tissue strength and flexibility, while also making it an attractive candidate for industrial applications. SA can be sourced from various brown algae species, such as *Ascophyllum nodosum*, *Laminaria hyperborea*, and *Macrocystis pyrifera*, as well as certain bacterial species, including *Azotobacter* and *Pseudomonas*. With a range of sources, brown algae-derived SA has established a significant market presence, it has become a valuable resource for diverse industries, driving innovation and development in fields such as food technology, pharmaceuticals, and personal care products [12-16].

The present study reports the facile preparation of cross-linked CA/SA bio composites via a solvent evaporation technique, to create a novel biomaterial. A range of analytical techniques was employed to characterize the prepared composites, Furthermore, antimicrobial analysis was conducted to determine the potential of the bio composites in resisting microbial growth and maintaining their integrity over time. By investigating the interplay between CA and SA, this research seeks to advance the development of sustainable biomaterials with improved performance and functionality.

MATERIALS AND METHODS

Materials: Sodium hydroxide pellets, hydrogen peroxide, acetic anhydride, glacial acetic acid, sulphuric acid, SA, distilled water were purchased from Molychem Laboratories, Mumbai.

Methodology: The formation of CA/SA Bio composite involves; simple mixing technique to obtain a homogeneous solution and followed by solvent evaporation technique to obtain the desired bio composites.

Synthesis of CA

Glacial acetic acid and cellulose were combined in a magnetic stirrer to activate the cellulose before initiating the processing of CA. Acetic anhydride and a few drops of sulfuric acid were added to the activated cellulose. The solution was continuously stirred in the magnetic stirrer to facilitate the acetylation process. Following acetylation, the solution was hydrolyzed using a mixture of glacial acetic acid and distilled water. The resulting solution was then filtered, rinsed with distilled water, and dried in a hot air oven.

Synthesis of CA/SA Bio composites

SA and CA were weighed in distinct weight ratios, such as 80:20 (CS1), 60:40 (CS2), 40:60 (CS3), and 20:80 (CS4). Each mixture was dissolved separately in distilled water and stirred thoroughly using a magnetic stirrer until the CA particles were fully dispersed. The prepared mixtures were then transferred to glass petri dishes. The evenly cast dishes were kept in an oven to evaporate the solvent, and finally, after the proper drying of the cast dishes, the CA/SA bio composites were allowed to cool down to room temperature. The prepared composites were then peeled off from the surface of the glass petri dishes.

CHARACTERIZATION

FTIR Analysis

The functional group and chemical structure were evaluated with a Perkin-Elmer-2000 spectrometer. Scans were collected for each spectrum at a resolution of 4 cm^{-1}, utilizing KBr pellets in the 4000–400 cm^{-1} range.

SEM analysis

Detailed surface data and high-resolution material photos are obtained using the scanning electron microscope (ZEISS). Images with the right resolution are obtained by scanning the specimen with an electron beam.

XRD analysis

XRD is a non-invasive method for inspecting a material's structure using X-rays. It can offer details about the chemical and physical characteristics, and crystal structure of a material. Using Cu kα radiation at 40 Kv and 40 mA, powder X-ray measurements were carried out on a Rigaku Ultima IV diffractometer in the 2θ = 5-80° range at a scanning rate of 10°/min

The average crystallite size was calculated using the Scherrer's formula,

$$D = {}^{K\lambda}/_{\beta cos\theta}$$

Where,

D→ Average crystallite size

K→ Scherrer constant

λ→ wavelength of the x-ray

β→ full width half maximum

θ→ Bragg angle of the diffraction peak

The percentage of crystallinity index was calculated using the formula,

$$CI\ (\%)\ = [\frac{Area\ of\ crystalline\ peaks}{Area\ of\ total\ peaks}] \times 100$$

Tensile strength

Using a Universal testing machine HT8503 at ASTM D638 to measure the tensile strength of resulting film was assessed.

Anti-microbial activity

Employing the Kirby-Bauer test, antibacterial activity was assessed. In the Kirby-Bauer test, antibiotic wafers, occasionally referred to as white discs, have been placed on a plate with bacteria or fungus grown on solid growth medium. Regions of clear media surround the discs following the bacteria or fungi were permitted to grow for 16–18 hours at 35–37 °C, implying that the antibiotic restricts the growth of the bacteria or fungi. Zones show how tested compounds stop microbes from growing on the cultured plates. To determine the antimicrobial viability, zones of inhibition were measured with an accurate ruler and compared to the control. The concentration of antibiotics that diffuse into the media reduces with distance from the source. The ensuing expansion of the clear zone of bacterium/fungus-free area surrounding the antibiotic-containing disc increases the susceptibility of the bacteria or fungi.

RESULTS AND DISCUSSION

FTIR Analysis

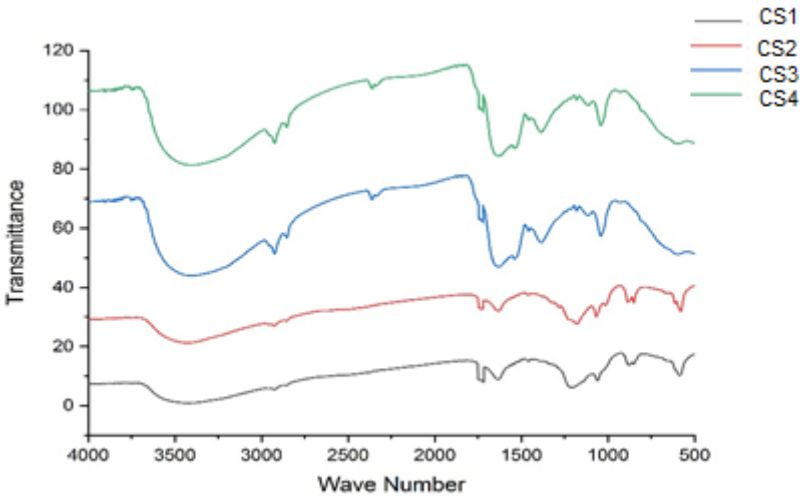

Fig 1: FTIR Spectra of CA/SA Bio composites

The FTIR spectra of CS1, CS2, CS3, and CS4 was displayed in figure 1. The spectra revealed characteristic absorption bands associated with both crosslinked CA and SA, albeit with certain variations across the samples. Broad absorption bands in the region of 3900–3300 cm^{-1} were attributed to the presence of free hydroxyl groups or residual moisture within the films. Peaks in the region of 2900–2800 cm^{-1} were associated with the C–H stretching vibrations of methyl groups. The absorption band within 1720–1750 cm^{-1} corresponded to the stretching of carbonyl (C=O) groups, while the deformation vibrations of methylene (CH_2) appeared in the 1650–1580 cm^{-1} range. Additionally, a peak observed around 1050–1030 cm^{-1} is attributed to the stretching vibrations of C–O bonds. Distinct peaks in the region of 1450–1545 cm^{-1} are assigned to carboxylate groups, while bands between 1200–1160 cm^{-1} correspond to C–O–C stretching vibrations. Peaks near 880–885 cm^{-1} indicated the presence of mannuronic acid units characteristic of SA, which were notably prominent in CS1 and CS2, reflecting their higher SA content. At the same region there was no prominent peaks for CS3 and CS4 reflected their comparatively lower SA content. Collectively, the FTIR spectral analysis confirms the successful crosslinking between cellulose acetate and sodium alginate chains.

SEM Analysis

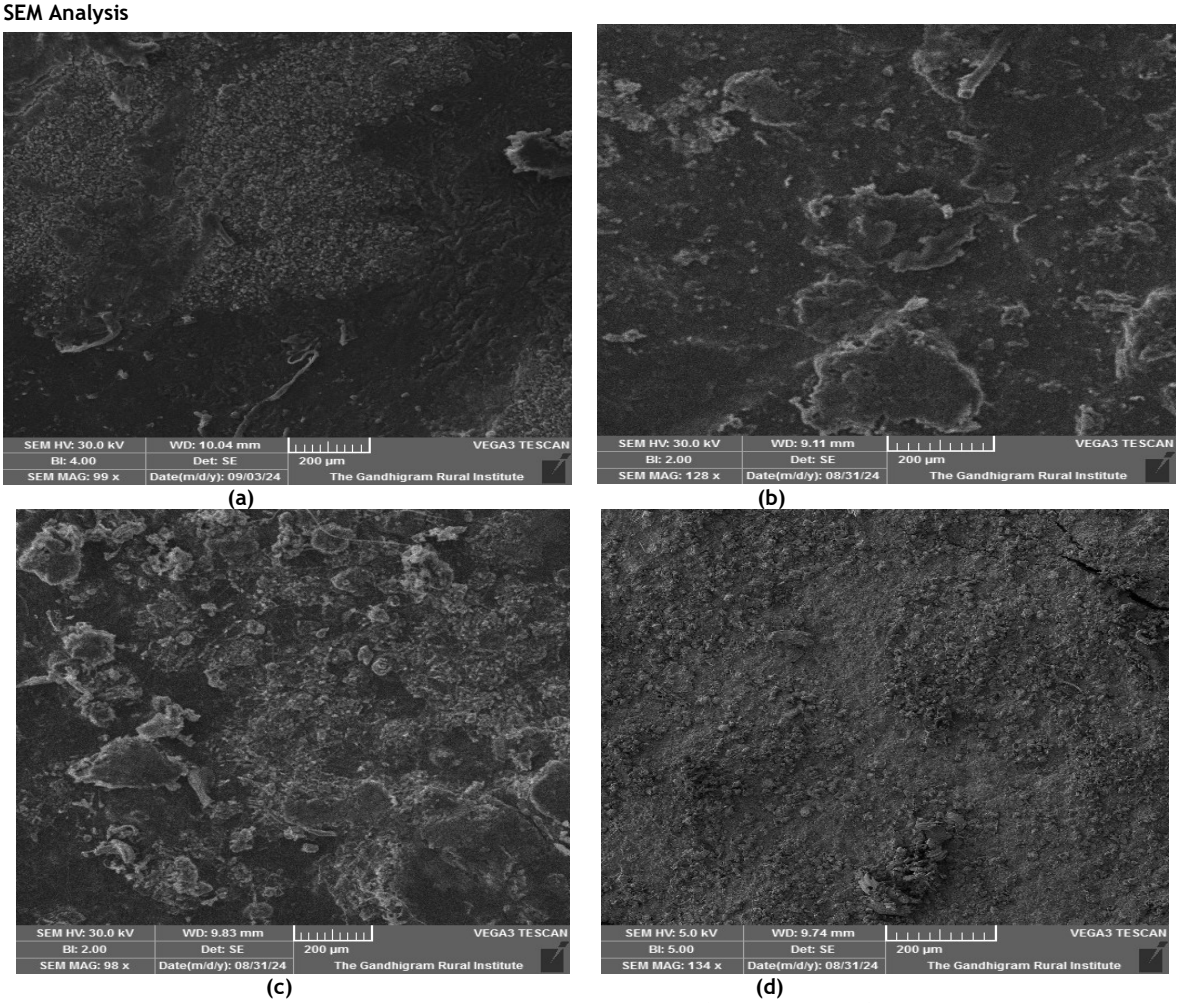

Fig 2: SEM images (a) CS1 (b) CS2 (c) CS3 (d) CS4

The surface morphology of the CS1, CS2, CS3, and CS4 films were analysed using SEM technique, as presented in Figure 2. CS1 and CS2 (fig.2(a) & 2(b)) exhibited comparable morphological characteristics, displaying relatively smooth and uniform surfaces typical of sodium alginate (SA). This characteristic SA morphology was clearly discernible in both samples. In CS2, dispersed cellulose acetate (CA) particles were evident within the SA matrix. As the CA content increased, its presence became more pronounced on the surface of the films. In CS3 and CS4 (fig.2(c)&2(d)), the typical SA morphology was markedly diminished, while the occurrence of CA particles became increasingly apparent. These morphological variations were attributed to compositional differences. SA, being water-soluble, readily dissolved to form a smooth surface, whereas CA, which is water-insoluble, tended to accumulate on the surface during film formation. Notably, this accumulation did not result in localised aggregation. Instead, CA particles were uniformly distributed across the surface, suggesting effective interpenetration and crosslinking between CA and SA. The even distribution of CA within the SA matrix contributed to the formation of homogenous composite films, as confirmed by SEM analysis.

XRD Analysis

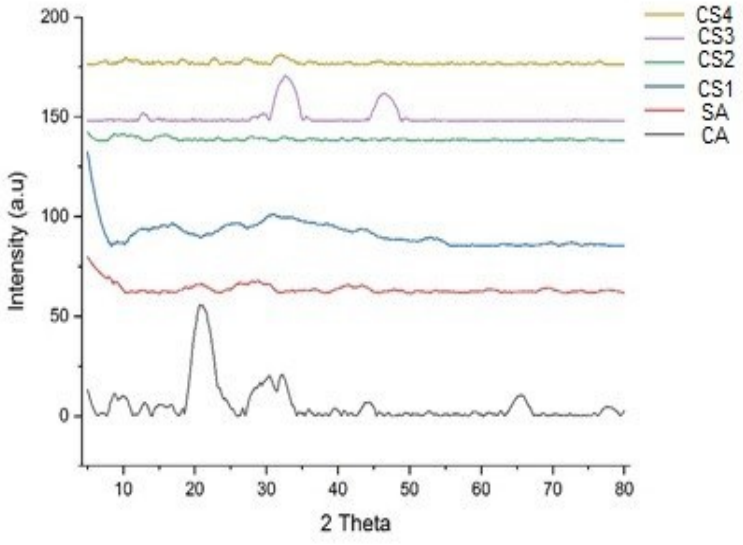

Fig 3: XRD Patterns of CA, SA, CS1, CS2, CS3, CS4

The XRD patterns of CA, SA, and their crosslinked composite films (CS1-CS4) exhibited distinctive features characteristic of both constituent polymers, albeit with notable variations in their diffractograms. Upon crosslinking, the CA and SA polymers displayed broad and weak diffraction peaks, which can be attributed to the formation of robust intermolecular and intramolecular hydrogen bonds between the polymeric chains. This phenomenon is indicative of a pronounced diminution in crystallinity, resulting from the crosslinking process. In the composite films (CS1-CS4), the characteristic peaks corresponding to the pristine CA and SA polymers were significantly attenuated or entirely eliminated, and only weak diffraction patterns were discernible, thereby underscoring the predominantly amorphous nature of these materials. The XRD pattern of CA revealed peaks at 2θ values of 20.99° and 16.15°, consistent with amorphous humps. The average crystallite size was calculated to be 0.526 nm, and the percentage of crystallinity index was determined to be 11.25%, thereby corroborating the amorphous nature of CA. For SA, the absence of discernible crystalline peaks further substantiated its amorphous morphology. As such, determination of crystallite size proved untenable, while the percentage of crystallinity index was found to be a mere 4.87%. The crosslinked composites CS1 to CS4 similarly evinced a lack of distinct peaks, affirming their amorphous architecture. The corresponding crystallinity indices for CS1, CS2, CS3, and CS4 were found to be 7.45%, 9.82%, 12.10%, and 14.10%, respectively. These results suggest a gradual augmentation in structural ordering with increasing CA content, while maintaining an overall amorphous character in the composite films.

Tensile strength

A comprehensive evaluation of the tensile strength of the prepared films was conducted. The tensile strength values for CS1, CS2, CS3, and CS4 were measured to be 3.27 N/mm², 3.09 N/mm², 2.50 N/mm², and 1.95 N/mm², respectively. A comparative analysis of these values indicated that CS1 possessed the highest tensile strength, implying its superior mechanical properties and potential for withstanding stress and strain. Consequently, CS1 emerged as the most suitable composition among the tested samples, demonstrating enhanced durability and applicability.

Antimicrobial activity

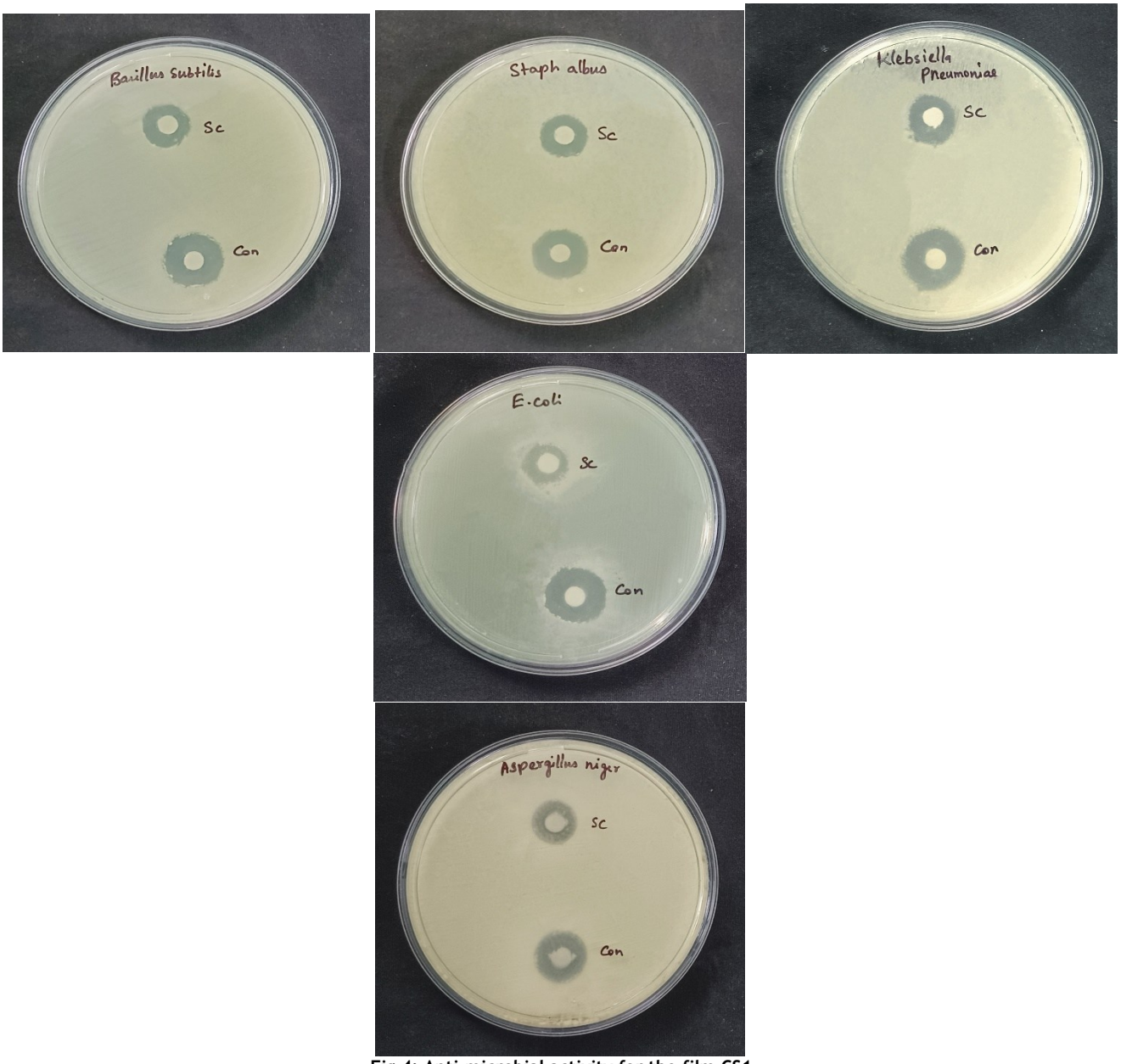

Fig 4: Anti-microbial activity for the film CS1

CS1 showed a higher tensile strength hence anti microbial activity was studied for it. The antimicrobial properties of film CS1 were assessed against various bacteria and fungi, with a control sample serving as a reference point. The results showed that CS1 had a lower zone of inhibition compared to the control, indicating moderate antimicrobial activity. Although cellulose acetate lacked inherent antimicrobial properties and sodium alginate had limited effects on microbial growth, the combination of both polymers in CS1 demonstrated enhanced antimicrobial characteristics, although it did not completely inhibit the growth of all microorganisms. The microbial analysis provided valuable insights into the antimicrobial properties of CS1 and its potential applications.

The microbial analysis revealed varying degrees of sensitivity among the tested microorganisms. *Klebsiella pneumoniae* exhibited the largest zone of inhibition, while *E. coli* displayed the smallest. Notably, both Gram-positive bacteria, including *Bacillus subtilis* and *Staphylococcus albus,* and Gram-negative bacteria showed sensitivity to CS1. Additionally, the fungus *Aspergillus niger* was also sensitive to CS1. These findings suggested that the film CS1 possessed broad-spectrum antimicrobial activity, although its efficacy varied depending on the type of microorganism.

CONCLUSION

The CA/SA bio composites were successfully prepared in four distinct ratios via solvent evaporation method. FTIR confirmed the cross-linking of CA and SA, which was further corroborated by XRD and SEM analysis. The XRD data revealed that all four compositions exhibited amorphous nature, with crystallinity indices indicating a predominantly disordered structure. The amorphous nature of the films contributed to their flexibility. Notably, the crystallinity index of SA was significantly enhanced upon the addition of CA. SEM analysis demonstrated uniform dispersion of CA on the SA surface, indicating excellent compatibility between the two polymers. The tensile strength of the films ranged from 1-4 N/mm^2, which was attributed to their amorphous nature. Nevertheless, the flexibility and insolubility of cellulose acetate in water make the prepared film an attractive candidate for delayed drug release techniques. Furthermore, the antimicrobial activity of CA was enhanced upon the addition of SA, suggesting a synergistic effect. These findings collectively demonstrate the biocompatibility and mutual enhancement of properties between CA and SA, yielding a film with excellent potential for diverse applications.

CONFLICT OF INTEREST

The authors declare that there is no conflict of interests regarding the publication of this article

REFERENCES

- D. Klemm , B. Heublein , H. P. Fink and A. Bohn ,(2005) Cellulose: Fascinating Biopolymer and Sustainable Raw Material *Angew. Chem., Int. Ed.*,44, 3358 – 3393 https://doi.org/10.1002/anie.200460587
- R. C. Law, Applications of cellulose acetate Cellulose acetate in textile application (2004) *Macromol. Symp.*,208 , 255 – 266 https://doi.org/10.1002/masy.200450410
- Heinze, Thomas & Liebert, Tim. (2012). Celluloses and Polyoses/Hemicelluloses. Polymer Science: A Comprehensive Reference, *Elsevier B.V.*,vol. 10, https://www.researchgate.net/publication/279997439_Celluloses_and_PolyosesHemicelluloses
- S. Fischer , K. Thümmler , B. Volkert , K. Hettrich , I. Schmidt and K. Fischer, (2008) Properties and Applications of Cellulose Acetate *Macromolecular Symposia*, vol. 262, 89-96. https://doi.org/10.1002/masy.200850210
- Jin, X.; Xu, J.; Wang, X.; Xie, Z.; Liu, Z.; Liang, B.; Chen, D.; Shen, G. (2014)Flexible TiO_2/cellulose acetate hybrid film as a recyclable photocatalyst. *RSC Adv*, *4*, 12640-12648. https://doi.org/10.1039/C3RA47710J
- Zulfiqar, S.; Rafique, U.; Akhtar, M.J. (2019) Removal of pirimicarb from agricultural wastewater using cellulose acetate–Modified ionic liquid membrane. *Environ. Sci. Pollut. Res* , *26*, 15795–15802. 10.1007/s11356-019-04681-6
- Barud, H.S.; de Araújo Júnior, A.M.; Santos, D.B.; de Assunção, R.M.N.; Meireles, C.S.; Cerqueira, D.A.; Rodrigues Filho, G.; Ribeiro, C.A.; Messaddeq, Y.; Ribeiro, S.J.L. (2008) Thermal behavior of cellulose acetate produced from homogeneous acetylation of bacterial cellulose. *Thermochim. Acta* , *471*, 61–69. http://dx.doi.org/10.1016/j.tca.2008.02.009
- Varshosaz, J.; Taymouri, S.; Jafari, E.; Jahanian-najafabadi, A.; Taheri, A. (2018) Formulation and characterization of cellulose acetate butyrate nanoparticles loaded with nevirapine for HIV treatment. *J. Drug Deliv. Sci. Technol.* *48*, 9–20. http://dx.doi.org/10.1016/j.jddst.2018.08.020
- Liakos, A.I.L.; Iordache, F.; Scarpellini, A.; Oneto, M.; Bianchini, P.; Grumezescu, A.M.; Holban, A.M. (2018) Cellulose acetate—Essential oil nanocapsules with antimicrobial activity for biomedical applications. *Colloids Surf. B Biointerfaces*, *172*, 471-479. https://doi.org/10.1016/j.colsurfb.2018.08.069
- Marrez, D.A.; Abdelhamid, A.E.; Darwesh, O.M. (2019) Eco-friendly cellulose acetate green synthesized silver nano-composite as antibacterial packaging system for food safety. *Food Packag. Shelf Life*, *20*, 100302. http://dx.doi.org/10.1016/j.fpsl.2019.100302
- Huda, E.; Rahmi; Khairan. (2019) Preparation and characterization of cellulose acetate from cotton. *IOP Conf. Ser. Earth Environ. Sci.*, *364*, 012021. 10.1088/1755-1315/364/1/012021
- Fertah M., Belfkira A., Dahmane E.-m., Taourirte M., Brouillette F. (2017) Extraction and characterization of sodium alginate from Moroccan Laminaria digitata brown seaweed. *Arab. J. Chem.* https://doi.org/10.1016/j.arabjc.2014.05.003
- Goh C.H., Heng P.W.S., Chan L.W. (2012) Alginates as a useful natural polymer for microencapsulation and therapeutic applications. *Carbohydr. Polym.* 88: 1-12. http://dx.doi.org/10.1016/j.carbpol.2011.11.012
- Phillips G.O., Williams P.A. (2009) *Handbook of Hydrocolloids*. CRC Press; Boca Raton, FL, USA http://dx.doi.org/10.1533/9781845695873
- Sachan N.K., Pushkar S., Jha A., Bhattcharya A. (2009) Sodium alginate: The wonder polymer for controlled drug delivery. *J. Pharm. Res.*:1191-1199. https://www.researchgate.net/publication/40773276_Sodium_alginate_The_wonder_polymer_for_controlled_drug_delivery
- Sellimi S., Younes I., Ben Ayed H., Maalej H., Montero V., Rinaudo M., Dahia M., Mechichi T., Hajji M., Nasri M. (2015) Structural, physicochemical and antioxidant properties of sodium alginate isolated from a Tunisian brown seaweed. *Int. J. Biol. Macromol.* https://doi.org/10.1016/j.ijbiomac.2014.10.016